Zeitschrift: Schweizerische mineralogische und petrographische Mitteilungen = Bulletin suisse de minéralogie et pétrographie

Band: 77 (1997)

Heft: 1

Artikel: Structural investigations along the join CaTiOSiO4-CaSnOSiO4

Autor: Kunz, Martin / Xirouchakis, Dimitros / Wang, Yanbin

DOI: https://doi.org/10.5169/seals-58464

SCHWEIZ. MINERAL. PETROGR. MITT. 77, 1–11, 1997

Structural investigations along the join $CaTiOSiO_4$–$CaSnOSiO_4$

by *Martin Kunz*[1], *Dimitrios Xirouchakis*[2], *Yanbin Wang*[3], *John B. Parise*[2] and *Donald H. Lindsley*[2]

Abstract

High resolution synchrotron X-ray data were used to structurally characterize a series of compounds along the solid-solution titanite (HT-phase)-malayaite. The refinements reveal a high sensitivity of the crystal symmetry on the amount of octahedral Sn present. This suggests a weak interaction between dipoles formed through Ti out-of-centre distortion. The structural evolution along the solid-solution also allows the identification of structural strain, which is caused by the geometrically competing arrangement of corner sharing octahedral chains occupied by Ti and Sn on one hand and edge sharing polyhedral chains occupied by Ca on the other hand. This strain is expressed in a systematic variation of structural parameters, such as Ti–O–Ti angles, Ca displacement parameters and Ca–O bond length distortion, as a function of octahedral occupation.

Keywords: titanite, malayaite, solid-solution, structural distortion, synchroton X-radiation, Rietveld analysis, KTP-phase.

Introduction

Titanite (sphene), $CaTiOSiO_4$, is an ubiquitous accessory mineral in igneous and metamorphic rocks, probably the most common titanium mineral other than ilmenite and rutile. It can participate in mineral-, mineral/melt- and mineral/fluid-equilibria that can be extremely sensitive to changes in intensive parameters such as pressure, temperature, oxygen fugacity and fluid composition (HUNT and KERRICK, 1977; WONES, 1989; MANNING and BOHLEN, 1991; XIROUCHAKIS and LINDSLEY, 1995; GIERÉ, 1992). In addition, because of the ability of titanite to retain certain radionucleids (e.g. uranium, thorium, radium), titanite based ceramics and glass-ceramics have been proposed as hosts for nuclear fuel waste (HAYWARD and CECHETTO, 1982; GASCOYNE, 1986). Thus, knowledge of the physicochemical properties of end-member titanite and solid solutions can help us to better understand the potential of this material in basic and applied research.

The crystal structure of titanite is dominated by corner sharing chains of TiO_6 octahedra running along the [100] axis and chains of edge sharing CaO_7 polyhedra parallel to [101]. These two chains are mutually connected by shared edges, leading to a dense polyhedral framework. Inserted in this framework are SiO_4 tetrahedra sharing corners with both TiO_6 octahedra and CaO_7 polyhedra. The structure undergoes a second-order $P2_1/a \leftrightarrow A2/a$ symmetry change either by heating above 220 °C (BISMAYER et al., 1992) or chemical substitution (OBERTI et al., 1991). In both cases it is mainly the position of the octahedral cation relative to the polyhedral centre which determines the phase transition (ZHANG et al., 1995). In $P2_1/a$, the Ti atom is placed off centre along the corner-linked octahedral chain while in A2/a, the octahedral metal is either in the centre of the oxygen octahedron or disordered on two opposite off centre positions, often leading to a domain texture within individual grains (SPEER and GIBBS, 1976). In fact, it is believed that the phase transition at 220 °C involves merely the loss of long range coherence between the individual off-centre dipoles, while locally the structure is still in a $P2_1/a$ state. True local A2/a symmetry is suggested to be

[1] High Pressure Group, European Synchrotron Radiation Facility, F-38043 Grenoble, France.
[2] Center for High Pressure Research and Department of Earth and Space Sciences, University at Stony Brook, Stony Brook NY 11794-2100, USA.
[3] Consortium for Advanced Radiation Sources, The University of Chicago, 5640 Ellis Ave., Chicago IL 60637, USA.

attained at a second phase anomaly around 580 °C (ZHANG et al., 1995). Due to the subtle nature of the mentioned phase transition, it was mainly the detailed investigation of this symmetry change, which motivated a large amount of crystallographic studies on titanite in the past (SPEER and GIBBS, 1976; TAYLOR and BROWN, 1976; GHOSE et al., 1991; OBERTI et al., 1991; HIGGINS and RIBBE, 1976; HIGGINS and RIBBE, 1977).

The Sn-analogue of titanite is known as the mineral malayaite ($CaSnOSiO_4$). Its structure is topologically identical to that of titanite (HIGGINS and RIBBE, 1977, GROAT et al., 1996). The main difference is found in the absence of an out-of-centre distortion on the octahedral site making therefore malayaite isostructural to the high-temperature phase of titanite.

The two minerals form a solid-solution at high temperature. At low-temperature TAKENUCHI (1971) proposed the existence of an asymmetric miscibility-gap with a critical point at 615 °C and $CaTi_{0.75}Sn_{0.25}OSiO_4$. However, new experiments suggest that this postulated gap, if present, may exist only at lower temperatures (XIROUCHAKIS and LINDSLEY, in prep.).

The detailed investigation of a series of compounds along the solid-solution would offer interesting insights into the structural evolution of a complicated framework structure in response to chemical substitution on a single site within the framework, complementing previous detailed studies on the $P2_1/a \leftrightarrow A2/a$ phase transition of the Ti end-member (TAYLOR and BROWN, 1976; SPEER and GIBBS, 1976; GHOSE et al., 1991; BISMAYER et al., 1992; ZHANG et al., 1995).

Another interesting aspect of this structure type evolves from the off-centre distortion of Ti atoms in the titanite low-temperature structure and has not attracted so much attention as yet. The out-of-centre distortion is characteristic for octahedrally coordinated d^0 metals (BURDETT, 1984; KANG et al., 1993; KUNZ and BROWN, 1995) and can induce non-linear optic effects in polar structures (LINES, 1991). In the $P2_1/a$ phase of titanite, the off centre vectors are oriented parallel to each other within an octahedral chain, but antiparallel within neighbouring chains. In contrast to the structurally similar and technically interesting $KTiOPO_4$ phase (KTP) (e.g. STUCKY et al., 1989), the $P2_1/a$ titanite phase is therefore centrosymmetric and does not exhibit any interesting non-linear optical properties.

It is not understood as yet why in KTP the Ti-off-centre vectors are arranged all parallel while in titanite they are only parallel within a chain, but antiparallel within neighbouring chains. A piece of information, which would help to understand this difference, is the nature of the interaction between individual off-centre dipoles. This is apparently different in titanite and KTP. One aid to an understanding of the mechanism of the dipole interaction is to investigate titanite- and KTP-compounds where the dipole-density is diluted by cations, which do not display the off-centre distortion at the octahedral site. This has been done for titanite to a certain extent in studies investigating natural titanites with a high degree of octahedral substitutions, i.e. mainly $((Al,Fe^{3+}) + (F,OH)) \leftrightarrow (Ti^{4+} + O^{2-})$ (HIGGINS and RIBBE, 1976; OBERTI et al., 1991). These studies reveal, that Al-substituted titanites remain $P2_1/a$ with up to 3 mol% Al on the octahedral site. Between 3 and 20 mol% Al substitution, $k + l = odd$ reflections characteristic of the $P2_1/a$ space group become streaked and eventually disappear when the structure adopts A2/a symmetry. Since the allovalent substitutions commonly found in natural titanite are always coupled substitutions, it is difficult to judge, to what extent the observed symmetry change is affected by the substitution on the anion-sites. Substitution on the anion site, however, might very well influence the dipole interaction between the octahedral Ti sites. In addition, it is likely that the natural samples investigated had different cooling histories and therefore may as well exhibit different ordering degrees, i.e. size of Ti/Al domains. The third caveat for using these studies to extract information about the dipole-interaction comes from the fact that the pure Al end-member vuagnatite ($CaAl(OH)SiO_4$) has a structure quite different from the titanite structure (OBERTI et al., 1991). This therefore induces further complications when looking only for effects caused by off-centre interactions.

All these ambiguities can be avoided by looking at titanite-like compounds with iso-valent substitutions whose end-member has a structure topologically identical to titanite. Also, it is advantageous to have the samples prepared at identical conditions, quenched from high temperatures to avoid ordering processes into large domains, thus ensuring a statistical distribution of the two octahedral cations on the available site. An ideal cation to substitute for Ti^{4+}, which fulfills the above mentioned criteria, is Sn^{4+}. Its ionic radius is similar to that of Ti^{4+} (SHANNON, 1976) and its crystal-chemical behaviour is therefore very similar to that of Ti^{4+}. A systematic study of titanite-malayaite solid solution (titanite quenched from high temperatures) may therefore reveal interesting information on the strength of the Ti dipole interaction, which can give rise to non-linear optic effects. A similar study on KTP is planed in order to compare the two different structure types.

Experimental procedure

SYNTHESIS

The titanite-malayaite solid solutions and the malayaite end-member were synthesized by reacting equimolar mixtures of $CaSiO_3$, TiO_2 (JMC 810420) and SnO_2 (JMC 18649). The $CaSiO_3$ used had been synthesized from a mechanical mixture of $CaCO_3$ (ALPHA lot 050980) and SiO_2 (JM S50389B). Both powders were dried at 400 °C (4 hrs) and 1000 °C (30 hrs) respectively, before weighing. Subsequently, the $CaCO_3$–SiO_2 mixture was ground in ethanol in an automatic agate mortar for 3 hrs. The mixture was slowly decarbonated over a period of 24 to 30 hrs (from 500 to 1000 °C) and then reacted at 1100 °C. During annealing, it was ground several times until optical examination and powder X-ray diffraction suggested that only wollastonite was present. The final product was stored in a desiccator. Prior to weighing the powders, $CaSiO_3$, TiO_2 and SnO_2 were dried in a Pt crucible at 1100 °C and 1000 °C for 5, 30 and 48 hrs respectively. After weighing, the mixtures were ground in an agate mortar with ethanol for two hours. Then they were reacted first at 1385 °C for 50 hrs and subsequently at 1200 °C to 1000 °C from 3 to 15 days in a Pt crucible with several thorough grinding cycles (2–3 hrs) during annealing. The second low-temperature annealing cycle was necessary in order to produce single-phase samples. Although this is not documented by previous careful experiments, it appears that a solid-liquid loop similar to many other silicate (e.g. Fe_2SiO_4–Mg_2SiO_4) or non-silicate systems exists in the $CaTiOSiO_4$–$CaSnOSiO_4$ join. This interfered with the high temperature synthesis of single phase samples with less than 40 mol% malayaite component. In all cases, mechanical mixtures were reacted at high temperature and then quenched by immersing the Pt crucible in a cold water bath. End member titanite (SphDX94-2) was synthesized by first reacting dry a $CaSiO_3$–TiO_2 mechanical mixture for 14 days at 1285 °C and at 1150 °C for 13 days with several cycles of thorough grinding between annealing. Subsequently, 0.6 grams from this powder were loaded with 50 ml H_2O in a Au capsule and reacted at 750 °C and 2 kbar for 7 days in a cold-seal pressure vessel.

Backscattered electron imaging and EDS analysis using a CAMEBAX electron microprobe confirmed the single phase nature of the powders as suggested by powder X-ray diffraction (CuKα radiation). Only traces of SiO_2, SnO_2 and/or $CaSiO_3$ were observed commonly in the interior of grains of single phase titanite-malayaite solid-solution.

In the following discussion, the samples will be labelled according to their Sn-content as MalXX, where XX denotes the percentage of Sn present ($100 \cdot Sn/(Sn + Ti)$).

X-RAY DIFFRACTION

The synthesis technique involving quenching from high temperature inhibited the growth of single crystals suitable for crystallographic analysis. Diffraction experiments therefore had to be done on powdered samples. Since the difference between $P2_1/a$ and A2/a is expressed in only very weak $k + l = odd$ reflections, it was crucial to have very high quality data. This was achieved by doing

Tab. 1 Experimental details of X-ray diffraction experiment:

	Mal00	**Mal10**	**Mal20**	**Mal40**	**Mal60**	**Mal80**	**Mal100**
a (Å)	7.06104(4)	7.05753(5)	7.06854(9)	7.08836(5)	7.11004(6)	7.13099(9)	7.15059(12)
b (Å)	8.71380(5)	8.73088(6)	8.75655(11)	8.78938(7)	8.82442(8)	8.85810(12)	8.89373(15)
c (Å)	6.55853(4)	6.57046(5)	6.58622(9)	6.60784(5)	6.62846(6)	6.64814(9)	6.66923(11)
β (°)	113.8084(5)	113.7113(3)	113.6559(6)	113.5736(4)	113.4929(5)	113.4201(7)	113.3332(9)
Volume (Å³)	369.196(4)	370.685(5)	373.428(9)	377.327(5)	381.310(6)	385.346(9)	389.446(11)
# of Refls.	542	267	274	276	279	283	286
# of points	4005	3982	7054	4778	3982	3932	4004
R_p (%)	3.88	3.87	4.34	3.50	3.47	6.09	5.07
R_{wp} (%)	5.54	5.13	5.79	4.53	4.59	8.34	6.27
R_{Fsq} (%)	4.01	4.88	4.07	2.88	3.33	4.24	4.04
$\sin\Theta/\lambda_{max}$	0.55	0.55	0.55	0.55	0.55	0.55	0.55
λ (Å)	0.6925(1)	0.6925(1)	1.1485(1)	0.6925(1)	0.6925(1)	0.6925(1)	0.6925(1)
Spacegroup	$P2_1/a$	A2/a	A2/a	A2/a	A2/a	A2/a	A2/a
Abs.-Corr.:	no	no	no	yes*	yes*	yes*	yes*
Soft-Constr.:	Si–O=1.64 Å	Si–O=1.64 Å	Si–O=1.64 Å	Si–O=1.64 Å	Si–O=1.64 Å	Si–O=1.64 Å	Si–O=1.64 Å

* as described by HEWAT (1979), ROUSE and COOPER (1970), LARSON and VON DREELE (1994)

Tab. 2 $k + l = odd$ reflections used as criteria to distinguish between $P2_1/a$ and $A2/a$. The intensities for these reflections were calculated for hypothetical $P2_1/a$ structures with the respective chemical composition using the program package GSAS (LARSON and VON DREELE, 1994).

	Mal10		Mal20		Mal40		Mal60		Mal80	
hkl	d (Å)	F^2	d (Å)	F^2	d (Å)	F^2	d (Å)	F^2	d (Å)	F^2
001	6.01	3.5	6.03	2.2	6.06	3.0	6.08	2.6	6.10	2.2
110	5.19	2.6	5.21	6.7	5.22	4.1	5.24	5.3	5.26	6.8
021	3.53	2.8	3.54	1.7	3.56	2.3	3.57	2.0	3.58	1.7
$12\bar{1}$	3.46	1.7	3.47	5.1	3.48	10.9	3.50	7.8	3.51	5.2
$11\bar{2}$	3.06	14.6	3.08	22.0	3.09	17.6	3.09	19.8	3.10	22.1
210	3.03	218.1	3.04	24.1	3.05	111.5	3.05	60.0	3.07	24.2
012	2.84	3.6	2.85	1.4	2.86	2.6	2.87	2.0	2.88	1.4
121	2.83	24.8	2.84	10.8	2.85	18.2	2.86	14.3	2.87	11.0
$22\bar{1}$	2.72	216.2	2.73	23.4	2.74	110.1	2.75	58.9	2.76	23.6
$21\bar{2}$	2.70	231.8	2.71	25.4	2.72	118.3	2.72	63.5	2.73	25.6
130	2.65	11.7	2.66	< 1	2.67	5.2	2.68	2.5	2.69	< 1
201	2.46	11.7	2.47	< 1	2.47	23.4	2.49	5.3	2.50	< 1

the experiments with synchrotron X-radiation on beamline X7a at the National Synchrotron Light Source (NSLS) in Brookhaven National Lab (BNL). Samples were loaded in a glass capillary of 0.4 mm diameter, which were rotated around their axis during data collection. The data were collected at a wavelength of 0.6925(2) Å (1.1149(2) Å for Mal20) selected from a channel-cut Ge(111) monochromator with a linear position-sensitive multiwire detector operating in the escape mode under a krypton gas pressure of 43 psi.

All refinements were carried out using the program package GSAS (Larson and VON DREELE, 1994). The datasets were first fitted using LeBail's method of intensity extraction (LEBAIL, 1992) while varying lattice parameters, zero-shift and peak-profile parameters. Backgrounds were fitted using a shifted Chebyschev function using 24 parameters (LARSON and VON DREELE, 1994). After convergence of the LeBail fit, peak-profile parameters and background coefficients were fixed before switching to Rietveld refinement of the structural parameters, i.e. lattice parameters, atomic coordinates as well as isotropic displacement parameters for Ca and Ti/Sn. The respective values for O and Si were kept fixed. In addition, a soft constraint of 1.64 Å (σ = 0.005, constraint-weight = 10) was applied on the rigid Si–O bonds, noting that this value was obtained in titanite as well as malayaite single crystal studies (SPEER and GIBBS, 1976; TAYLOR and BROWN, 1976; GHOSE et al., 1991; HIGGINS and RIBBE, 1977). These constraints helped to avoid correlation problems during refinement. As indicated on table 1, an absorption-correction was applied to samples Mal40, Mal60, Mal80 and Mal100. The absorption for the cylindrical samples was calculated according to an empirical exponential formula (HEWAT, 1979; ROUSE and COOPER., 1970; LARSON and VON DREELE, 1994).

To distinguish between the two space groups, we relied on the $k + l = odd$ reflections characteristic for the $P2_1/a$ space group. For each composition, a theoretical powder pattern was calculated in $P2_1/a$ using the given wavelength. From the calculated pattern, the strongest $k + l = odd$ reflections within the available $\sin\Theta/\lambda$-range were selected as criteria for the spacegroup (Tab. 2). If these reflections were absent, the refinement was proceeded in spacegroup A2/a. In the final stage of the refinement, peak-profile parameters as well as background parameters were added to be varied together with the structural parameters. The results of the Rietveld refinement are given in table 3.

TEM

Small amounts of the Mal10 sample was crushed in alcohol and the dispersed fine powder was collected on a "Holey carbon grid". Observations were carried out using a Jeol 200 CX transmission electron microscope operating at 200 kV. The samples appear to be well crystallized, although a small amount of glass is present in the sample which may be due to the first synthesis stage at 1400 °C.

Results and discussion

Unit cell data and atomic coordinates for the refinements are given in table 1 and table 3, respec-

Tab. 3 Results of Rietveld refinement:

		x	y	z	U_{iso}(Å^2)
Ca	**Mal00**	0.2425(7)	0.1671(2)	0.0017(8)	0.0058(5)
	Mal10	1/4	0.1674(1)	0	0.0075(5)
	Mal20	1/4	0.1674(2)	0	0.0111(8)
	Mal40	1/4	0.1665(2)	0	0.0140(7)
	Mal60	1/4	0.1652(2)	0	0.0179(7)
	Mal80	1/4	0.1637(3)	0	0.0100(12)
	Mal100	1/4	0.1629(2)	0	0.0186(8)
Ti/Sn	**Mal00**	0.5162(4)	0.0029(5)	0.4988(5)	0.0010(3)
	Mal10	1/2	0	1/2	0.0018(2)
	Mal20	1/2	0	1/2	0.0008(4)
	Mal40	1/2	0	1/2	0.0024(4)
	Mal60	1/2	0	1/2	0.0066(2)
	Mal80	1/2	0	1/2	0.0038(3)
	Mal100	1/2	0	1/2	0.0081(7)
Si	**Mal00**	0.7517(8)	0.1831(2)	0.9994(1)	0.0025*
	Mal10	3/4	0.1829(2)	0	0.0025*
	Mal20	3/4	0.1821(3)	0	0.0025*
	Mal40	3/4	0.1820(2)	0	0.0025*
	Mal60	3/4	0.1814(2)	0	0.0025*
	Mal80	3/4	0.1827(5)	0	0.0025*
	Mal100	3/4	0.1811(3)	0	0.0025*
O1	**Mal00**	0.751(2)	0.0709(4)	0.493(2)	0.005*
	Mal10	3/4	0.0722(4)	1/2	0.005*
	Mal20	3/4	0.0712(5)	1/2	0.005*
	Mal40	3/4	0.0761(4)	1/2	0.005*
	Mal60	3/4	0.0798(4)	1/2	0.005*
	Mal80	3/4	0.0843(7)	1/2	0.005*
	Mal100	3/4	0.0850(5)	1/2	0.005*
O2	**Mal00**	0.909(1)	0.0652(9)	0.185(1)	0.005*
	Mal10	0.9123(3)	0.0659(2)	0.1828(3)	0.005*
	Mal20	0.9118(4)	0.0660(3)	0.1832(4)	0.005*
	Mal40	0.9117(3)	0.0648(2)	0.1791(3)	0.005*
	Mal60	0.9141(4)	0.0655(2)	0.1770(3)	0.005*
	Mal80	0.9142(6)	0.0663(4)	0.1733(6)	0.005*
	Mal100	0.9136(4)	0.0677(3)	0.1755(4)	0.005*
O2a	**Mal00**	0.382(1)	0.212(1)	0.398(2)	0.005*
O3	**Mal00**	0.382(1)	0.210(1)	0.394(2)	0.005*
	Mal10	0.3817(3)	0.2122(2)	0.3956(4)	0.005*
	Mal20	0.3814(4)	0.2114(3)	0.3975(5)	0.005*
	Mal40	0.3793(4)	0.2127(3)	0.3948(4)	0.005*
	Mal60	0.3777(4)	0.2141(3)	0.3930(4)	0.005*
	Mal80	0.3774(7)	0.2147(5)	0.3918(7)	0.005*
	Mal100	0.3740(5)	0.2124(3)	0.3920(5)	0.005*
O3a	**Mal00**	0.9132(9)	0.3173(9)	0.434(1)	0.005*

tively. Figure 1 shows Rietveld plots of Mal00 and Mal10.

The presented series of experiments reveals that already at a Sn concentration of 10%, even with high signal/background synchrotron radiation, no $k + l = odd$ reflections can be observed anymore.

This finding suggests that at a Sn content ≤ 10%, the domains formed by coherent Ti off-centre distortion are smaller than the transversal coherence length of the X-rays (≈ 1 μm) used to probe the structure. Randomly replacing as little as 10% of the octahedral Ti^{4+} by Sn^{4+} seems thus to lead to a complete loss of the Ti out-of-centre coherence. This finding is supported by a TEM experiment on Mal10: The only domain structures observed in this experiment were very weak and of a typical domain-size of 0.1 mm. These dimen-

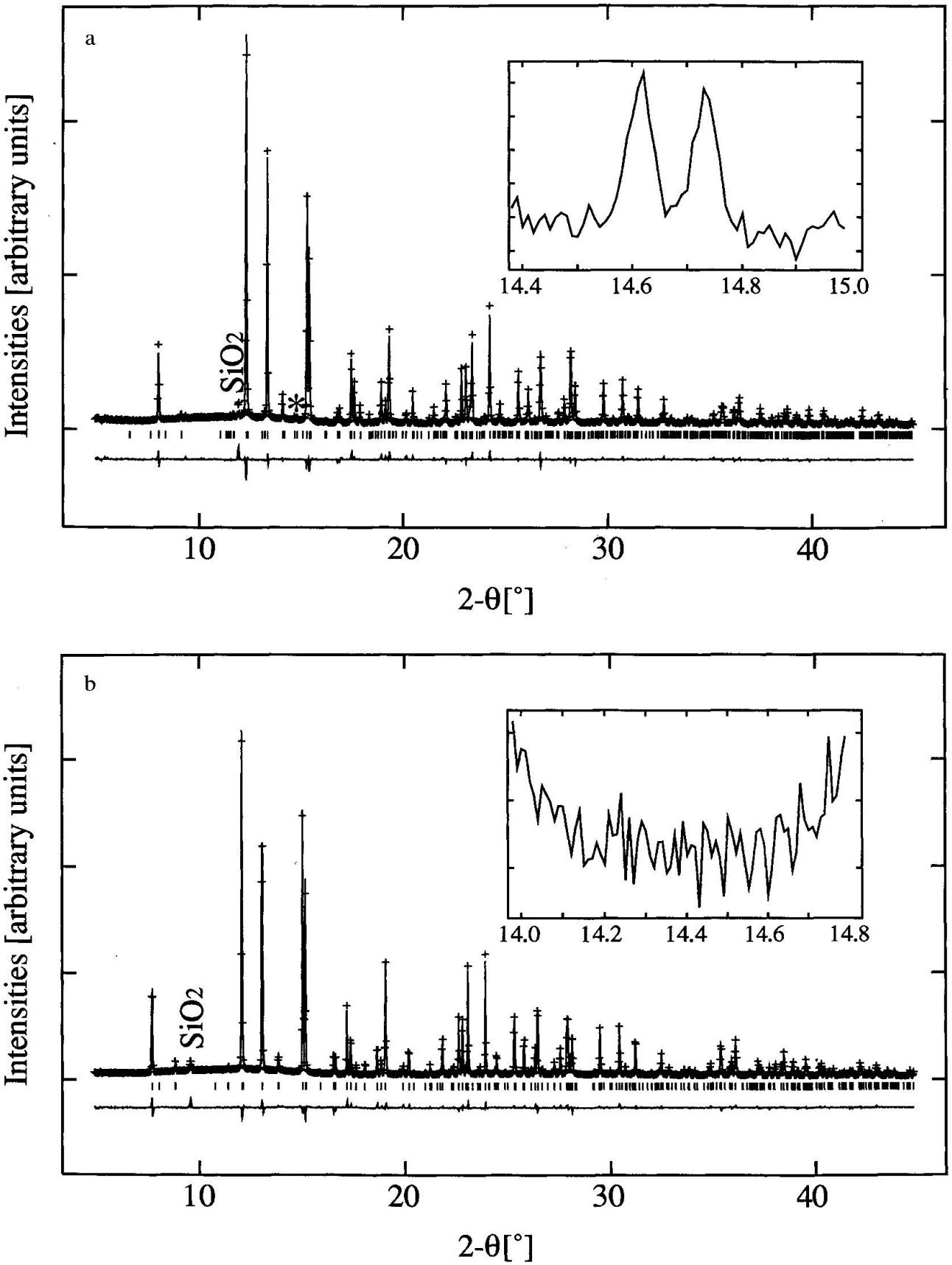

Fig. 1 Rietveld plots of Mal00 (a) and Mal10 (b), respectively. The peaks labeled with SiO_2 are due to quartz (a) and cristobalite (b) respectively. The insets show an enlargement of the area where the strongest non-overlapping $P2_1/a$ specific peaks ($22\bar{1}$ and $21\bar{2}$) are expected. These two peaks are also marked with a star in figure 1a. Their absence in figure 1b indicates space-group A2/a. These peaks were observed only in Mal00.

sions are well above the X-ray coherence length and can therefore not evoke the observed A2/a symmetry through spatial averaging over domains with coherent Ti distortion vectors. That the out-of-centre dipole orientation is indeed truly disordered is demonstrated by a selected-area diffraction (SAED) pattern (Fig. 2). This contains fundamental reflections of the 020, $\bar{1}02$, and $\bar{1}22$ types. Reflections hkl, with $k + l = odd$, which are characteristic of the $P2_1/a$ spacegroup, are absent. In fact, no k + l = odd reflections could be found during TEM observations. In view of the very small transversal coherence length ($\approx$ 50 nm) of an electron beam, we conclude therefore, that in Mal10 the dipole vectors are randomly oriented parallel or antiparallel to the octahedral chain axis.

The loss of a long range coherence of the distortion vector due to such a small perturbation implies an only small dipole interaction between neighbouring Ti atoms. This conclusion is in accordance with previous findings on natural titanites, where the presence of impurities on the octahedral site leads to the same symmetry change (OBERTI et al., 1991). A weak interaction between neighbouring Ti dipoles suggests the possibility to modify the structure of titanite in such a way that the Ti out-of-centre vectors are all oriented parallel in a similar manner as it is observed in KTP. This might be achieved by chemical substitution or the application of an external electric field during crystal synthesis. The possibility to artificially convert the titanite structure into an acentric spacegroup is supported by the mineral tilasite

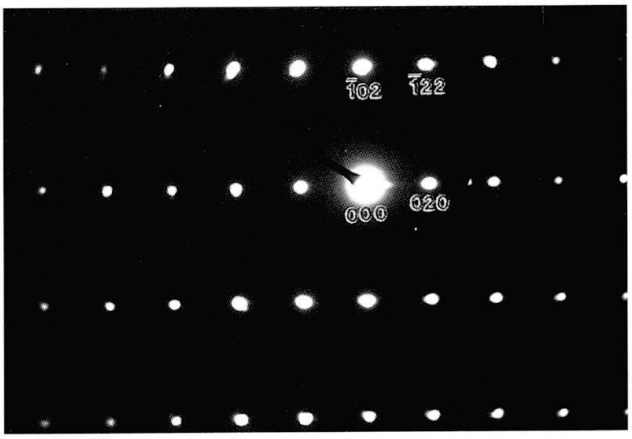

Fig. 2 Selected-area electron diffraction (SAED) pattern of a Mal10 crystal. Note the absence of the $k + l = odd$ reflections (such as 112) indicating space group A2/a.

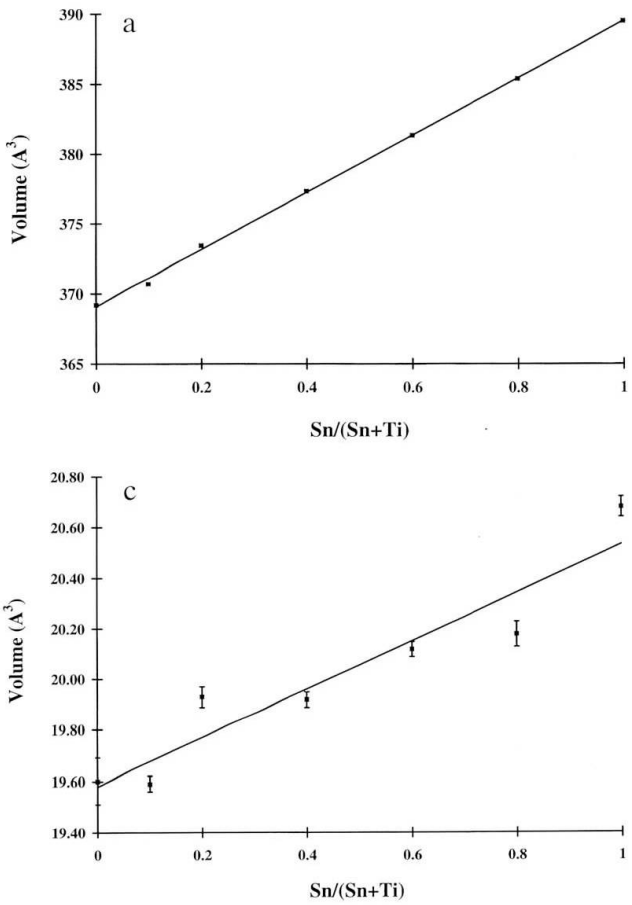

Fig. 3 Volumes as a function of Sn-content. Polyhedral volumes were calculated with the program "volcal" by L. Finger and Y. Ohashi (http://www.lmcp.jussieu.fr/sincris/logiciel/prg-volcal.html). Solid lines represent linear regression fits through data.
a) unit cell volume (R^2 = 0.999), error bars are smaller than symbols; b) octahedral volume (R^2 = 0.97), c) Ca polyhedral volume (R^2 = 0.90).

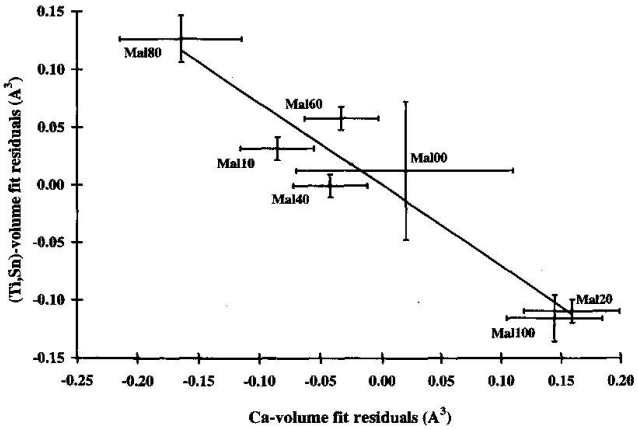

Fig. 4 Residuals of linear regressions through Ca-polyhedral and octahedral volumes, respectively. The strong correlation is shown by the R^2 of 0.96 of a linear regression through the data points.

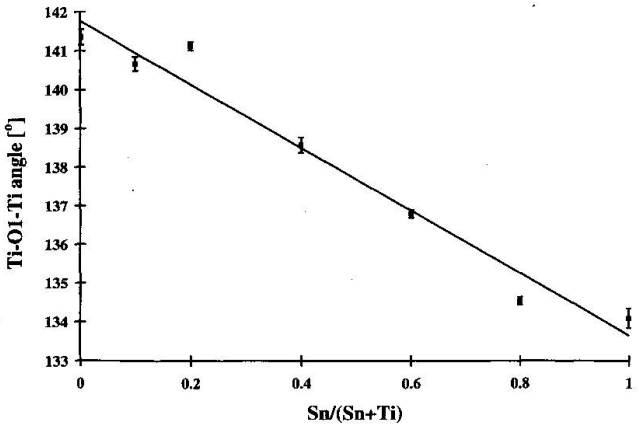

Fig. 5 Pivot-angle (Ti–O1–Ti) of the octahedral chains as a function of Sn-content. The decreasing trend reflects steric strain within the structure. This effect is partly compensating for the octahedral volume increase which is in competition to the geometric requirements of the Ca-chains. The line serves as a guide to the eye.

($CaMgF(AsO_4)$), which is topologically very similar to titanite and malayaite (BLADH et al., 1972), but crystallizes in the acentric spacegroup Cc and exhibits a measurable piezoelectric effect (SMITH and PRIOR, 1911). It is notable, that in the MgO_4F_2-octahedra of tilasite, the distortion vector are oriented perpendicular to the octahedral chain axis, rather than parallel to it as in titanite!

The present study also allows to discuss the structural changes induced in a mineral by chemical substitution on a single site, while preserving the bonding topology:

As expected, the replacement of Ti by Sn leads to a gradual increase in cell volume and octahedral site volume (Figs 3a and 3b). As predicted by HIGGINS and RIBBE (1977), this is paralleled by a continuing increase of the volume of the CaO_7 polyhedron (Fig. 3c). This is explained by the steric constraints between the Ti/Sn octahedra and the CaO_7 polyhedra induced by the tight connection between these two structural units. It is interesting to note that the scattering of the observed Ca and Ti/Sn volumes around their respective linear regression line shows a significant negative correlation (Fig. 4). This indicates a strong correlation of the two volumes during structure refinement. Due to the above mentioned tight interlacing of CaO_7 and Ti/SnO_6 polyhedra, a small change in atomic coordinates of the oxygen atoms has a significant but opposite effect on the two volumes. It is noteworthy that this is not a problem inherent to Rietveld analysis, but can also be observed when comparing polyhedral volumes of different titanite single crystal studies found in the literature (XIROUCHAKIS et al., 1996). The use of polyhedral volumes for crystal-chemical arguments is therefore rather questionable for those cases where the structure consists of a densely packed arrangement of polyhedra.

There is more evidence for the existence of a considerable amount of steric strain in the titanite topology.

(1) Si–O bond lengths (SPEER and GIBBS, 1976; GHOSE et al., 1991; TAYLOR and BROWN, 1976; HIGGINS and RIBBE, 1976; HIGGINS and RIBBE, 1977) are longer (1.64 Å) than a typical Si–O bond for silicates (1.61 Å) (KUNZ and ARMBRUSTER, 1990) leading to a rather atypical underbonding of the SiO_4 tetrahedra. This suggests, that in titanite the otherwise very dominant Si–O bonds are not able to fully overcome the rigidness of the CaO_7–TiO_6 framework.

(2) The Ti–O1–Ti angle at the corner-sharing oxygen of the octahedral chain decreases with increasing Sn-content (Fig. 5). This can be viewed as a response to the increasing mismatch between the dimensions of the octahedral chain and the CaO_7 chain, which are mutually interconnected.

In apparent contradiction to the increasing Ca–O bond-lengths with increasing Sn content, the bond valence sum of the Ca atoms remains almost constant through the whole series of compounds investigated (Tab. 4). An increase in average bond length for a given cation suggests rather an increasing underbonding of the respective cation. The deviation from this rule can be explained by the distortion theorem (BROWN, 1992), stating that for a given average bond length, the bond-valence sum will be higher for more distorted bonding arrangements than for a set of equal bond lengths. That this theorem indeed applies in this case can be seen in the variance of the Ca–O

Tab. 4 Bond valence sums for cations of the samples investigated. The bond valence sum of the octahedral cation is calculated by forming the proportional average of the values for a full Ti and Sn occupation respectively (x = Sn/(Sn + Ti)). Values for Si are omitted because their bond-lengths were soft-constrained during refinements.

	Ca (v.u.)	x(Sn) + (1–x)(Ti) (v.u.)
Mal00	1.98	4.15
Mal10	1.98	4.14
Mal20	1.92	4.01
Mal40	1.96	4.14
Mal60	1.95	4.11
Mal80	1.95	4.08
Mal100	1.88	4.21

bonds along the join (Fig. 6). There is a clear increase of the bond-length variance when going from Mal20 to Mal100. This shows an increasing coordination distortion of the CaO_7 polyhedron along the titanite-malayaite solid-solution, induced by the sterically driven increase of the volume of the CaO_7 polyhedron.

As shown by previous single crystal studies (TAYLOR and BROWN, 1976; GHOSE et al., 1991; HIGGINS and RIBBE, 1976; HIGGINS and RIBBE, 1977; GROAT et al., 1996), the displacement parameter for the Ca position in titanite as well as malayaite is strongly elongated roughly along the a-axis. This elongation of the thermal ellipsoid was interpreted as being an artefact due to the domain growth in natural titanites (SPEER and GIBBS, 1976). The fact that the same kind of elongation is also observed in pure malayaite (HIGGINS and RIBBE, 1977; GROAT et al., 1996) however does not

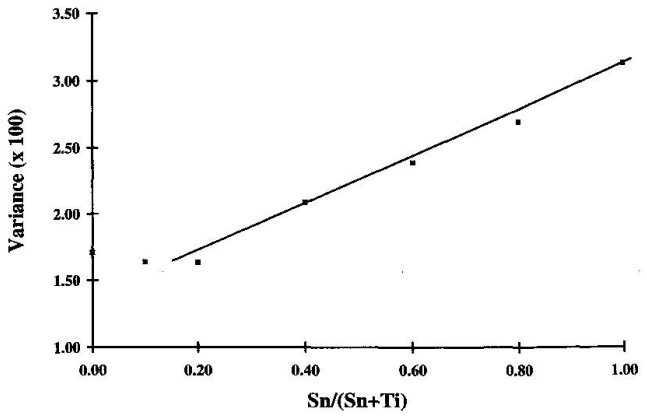

Fig. 6 Variance of Ca–O bond lengths as a function of Sn-content. Note the marked increase of the variance with increasing Sn-content, i.e. increasing Ca-polyhedral volume, indicating a stronger distortion of the Ca-polyhedron for Sn-rich samples. The line serves as a guide to the eye.

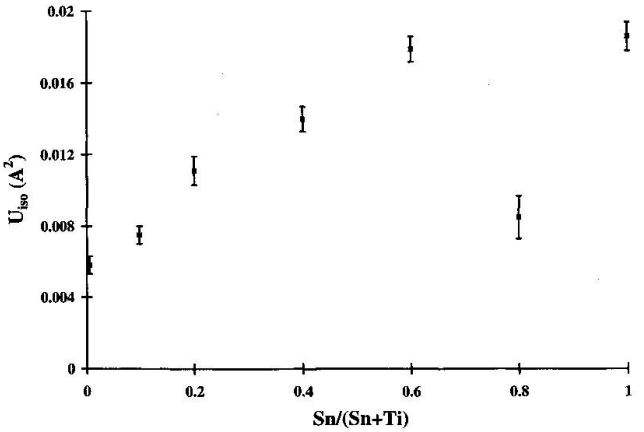

Fig. 7 Isotropic displacement parameters (Å^2) of Ca as a function of Sn-content. The increasing trend for higher Sn-contents and thus Ca-polyhedral volume is interpreted as a manifestation of a flatter potential well due to the sterically caused stretching of the Ca-site.

support such an interpretation since pure malayaite is not exhibiting strong domain growth due to the absence of domain inducing out-of-centre distortions on the octahedral site (GROAT et al., 1996). The observed elongation is therefore rather due to a flat potential minimum, probably due to the sterically driven extension of the CaO_7 polyhedron along the a-axis, which is also the direction of the octahedral chain. A replacement of Ti with the larger Sn on the octahedral site is therefore expected to distort this site even further, leading to even larger displacement parameters. This can be observed from careful refinements of the Ca displacement parameters. Such values obtained from Rietveld refinement have to be interpreted carefully, since they are very susceptible to correlation problems between the individual parameters. By fixing the displacement parameters of the light scatterers (i.e. O and Si), we assume that values for refined U_{iso}(Ca) are self-consistent, even if they may not be accurate on an absolute scale. The values obtained show a clear trend towards an increase of U_{iso}(Ca) with increasing Sn content (Fig. 7). The value for Mal80 is obviously not obeying this trend. The reason for this outlier is not clear, and might be due to the mentioned correlation problems.

The observed increase of the Ca thermal parameters as a function of Sn-content does not allow to distinguish between a dynamic and a static disorder of the Ca-atoms. This could most precisely be done with a temperature dependent single crystal x-ray diffraction experiment on a malayaite sample. However, close examination of the CaO_7 bond lengths from our data seems to favour a static displacement: As shown in table 4,

the observed polyhedral distortion of CaO_7 does not quite satisfy the bond valence requirements for Ca^{2+} in Mal100. A statically disordered Ca site, however, would locally increase the bond-length distortion, thus leading to a higher bond-valence sum, which would fulfill the valence requirements of Ca^{2+}.

Conclusion

– The coherence between Ti out-of-centre distortion vectors is lost already at a small perturbation (Sn-concentration 10%), suggesting an only very weak long-range interaction between dipole vectors.

– The topology of the titanite and malayaite structure with interlaced Ti/SnO_6 and CaO_7 polyhedral chains induces strong steric constraints depriving the SiO_4 tetrahedra from their otherwise dominant role as structural unit.

– When arranged in extended arrays, the usually weakly bonding Ca can act as a significant structural unit even in silicate structures.

Acknowledgements

Dave E. Cox' help was crucial in getting the Synchrotron X-ray experiment done. He also significantly contributed to this work in the form of stimulating discussions. The TEM observations were carried out at the Scanning/Transmission Electron Microscope Laboratory at Stony Brook, supervised by R.J. Reeder. DHL acknowledges support from NSF grant #EAR9304699. JBP's work is supported by NSF grant #EAR9506483. Constructive reviews from U. Bismayer and K. Lengauer helped to improve the manuscript. CHiPR is an NSF-funded science and technology centre; MPI contribution No. 194.

References

BISMAYER, U., SCHMAHL, W., SCHMIDT, C. and GROAT, L.A. (1992): Linear birefringence and X-ray diffraction studies of the structural phase transition in titanite, $CaTiSiO_5$. Phys. Chem. Mineral. 19, 260–266.

BLADH, K.W., CORBETT, R.K., MCLEAN, W.J. and LAUGHON, R.B. (1972): The crystal structure of tilasite. Amer. Mineral., 57, 1880–1884.

BROWN, I.D. (1992): Chemical and steric constraints in inorganic solids. Acta Crystallogr. B48, 553–572.

BURDETT, J.K. (1984): From bonds to bands and molecules to solids. Progr. Sol. State Chem. 15, 173–255.

GASCOYNE, M. (1986): Evidence for the stability of the potential nuclear waste host, sphene, over geological time, from uranium-lead ages and uranium-series measurements. Appl. Geochem., 1, 199–210.

GHOSE, S., ITO, Y. and HATCH, D.M. (1991): Paraelectric-antiferroelectric phase transition in titanite, $CaTiSiO_5$; I. A high temperature X-ray diffraction study of the order parameter and transition mechanism. Phys. Chem. Mineral., 17, 591–603.

GIERÉ, R. (1992): Compositional variation of metasomatic titanite from Adamello (Italy). Schweiz. Mineral. Petrogr. Mitt., 72, 167–177.

GROAT, L.A., KEK, S., BISMAYER, U., SCHMIDT, C., KRANE, H.G., MEYER, H., NISTOR, L. and TENDELOO, G.V. (1996): A synchrotron radiation, HRTEM, X-ray powder diffraction, and raman spectroscopic study of malayaite, $CaSnSiO_5$. Amer. Mineral., 81, 595–602.

HAYWARD, P. and CEHETTO, E. (1982): Development of sphene-based glass ceramics tailored for Canadian waste disposal conditions. In: TOPP, S., (ed.): Scientific Basis for Nuclear Waste Management, Vol. 3, 91–98.

HEWAT, A.W. (1979): Absorption corrections for neutron diffraction. Acta Crystallogr., A35, 248–250.

HIGGINS, J.B. and RIBBE, P.H. (1976): The crystal chemistry and space groups of natural and synthetic titanites. Amer. Mineral., 61, 878–888.

HIGGINS, J.B. and RIBBE, P.H. (1977): The structure of malayaite, $CaSnOSiO_4$, a tin analogue of titanite. Amer. Mineral., 62, 801–806.

HOWARD, C.J. (1982): The approximation of asymmetric neutron powder diffraction peaks by sums of gaussians. J. Appl. Crystallogr., 15, 615–620.

HUNT, J. and KERRICK, D. (1977): The stability of sphene: experimental redetermination and geologic implications. Geochim. Cosmochim. Acta, 41, 279–288.

KANG, S.K., TANG, H. and ALBRIGHT, T.A. (1993): Structures of d^0 ML_6 and ML_5 complexes. J. Amer. Chem. Soc., 115, 1971–1981.

KUNZ, M. and ARMBRUSTER, T. (1990): Difference displacement parameters in alkali feldspars: Effects of (Si, Al) order-disorder. Amer. Mineral., 75, 141–149.

KUNZ, M. and BROWN, I.D. (1995): Out-of-center distortions around octahedrally coordinated d^0 transition metals. J. Sol. State Chem., 115, 395–406.

LARSON, A.C. and VON DREELE, R.B. (1994): GSAS, General Structure Analysis System. Los Alamos National Laboratory, LAUR 86-748.

LEBAIL, A. (1992): Extracting structure factors from powder diffraction data by iterating full pattern profile fitting. In: PRINCE, E. and STALIEK, J.K. (eds): Accuracy in powder diffraction II, Special Publication 846, p. 213. National Institute of Standards and Technology, Gaithersburg. Maryland.

LINES, M. (1991): Influence of d-orbitals on the non-linear optical response of transparent transition-metal oxides. Phys. Rev. B, 43(14), 11978–11990.

MANNING, C. and BOHLEN, S. (1991): The reaction titanite + kyanite = anorthite + rutile and titanite-rutile barometry in eclogites. Contrib. Mineral. Petrol., 109, 1–9.

OBERTI, R., SMITH, D.C., ROSSI, G. and CAUCIA, F. (1991): The crystal chemistry of high-aluminum titanites. Eur. J. Mineral., 3, 777–792.

ROUSE, K.D. and COOPER M.J. (1970): Absorption corrections for neutron diffraction. Acta Crystallogr., A26, 682–691.

SHANNON, R. (1976): Revised effective ionic radii and systematic studies of interatomic distances in halides and chalcogenides. Acta Crystallogr., A32, 751–767.

SMITH, G.F.H. and PRIOR, G.T. (1911): On fermorite, a new arsenate and phosphate of lime and strontia and tilasite, from the manganese-ore deposits of India, Mineral. Mag., 16, 84–96.

SPEER, J.A. and GIBBS, G. (1976): The crystal structure of synthetic titanite, $CaTiOSiO_4$, and the domain tex-

tures of natural titanites. Amer. Mineral., 61, 238–247.

STUCKY, G.D., PHILIPS, M.L. and GIER, T.E. (1989): The potassium titanyl phosphate structure field: A model for new non-linear optical materials. Chem. Mater., 1, 492–509.

TAKENUCHI, S. (1971): Hydrothermal synthesis and consideration of the genesis of malayaite. Mineral. Depos., 6, 335–347.

TAYLOR, M. and BROWN, G.E. (1976): High-temperature structural study of the $P2_1/a \leftrightarrow A2/a$ phase transition in synthetic titanite, $CaTiSiO_5$. Amer. Mineral., 61, 435–447.

THOMPSON, P., COX, D. and HASTINGS, J. (1987): Rietveld refinement of Debye-Scherrer synchrotron X-ray data from Al_2O_3. J. Appl. Crystallogr., 20, 79–83.

WONES, D. (1989): The petrologic significance of the assemblage titanite + magnetite + quartz in granitic rocks. Amer. Mineral., 74, 744–749.

XIROUCHAKIS, D., KUNZ, M., PARISE, J.B. and LINDSLEY, D.H. (subm.): Synthesis methods and unit cell volume of end member titanite ($CaTiOSiO_4$). Amer. Mineral.

XIROUCHAKIS, D. and LINDSLEY, D.H. (1995): Low pressure equilibria among titanite (sphene), hedenbergite, iron-titanium oxides and silica: experiments and internally consistent thermodynamic data for titanite. In: V.M. Goldschmidt Conference, Programs with Abstract, Penn. State.

ZHANG, M., SALJE, E., BISMAYER, U., UNRUH, H., WRUCK, B. and SCHMIDT, C. (1995): Phase transition(s) in titanite $CaTiSiO_5$: An infrared spectroscopic, dielectric response and heat capacity study. Phys. Chem. Mineral., 22, 41–49.

Manuscript received July 22, 1996; revised manuscript accepted October 31, 1996.